

Aus dem Institut für Klinische Pharmakologie und Toxikologie
der Medizinischen Fakultät Charité – Universitätsmedizin Berlin

DISSERTATION

**Investigation of the transcriptional regulation and function of TFF1
in female reproductive organs**

zur Erlangung des akademischen Grades
Doctor rerum medicarum (Dr. rer. medic.)

vorgelegt der Medizinischen Fakultät
Charité – Universitätsmedizin Berlin

von

Enhong Zhong

aus Jiangxi, China

Gutachter/in: 1. Prof. Dr. med. G. Schoenfelder
 2. Prof. Dr. med. M. van der Giet
 3. Prof. Dr. rer. nat. O. Huber

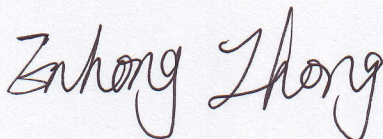
Datum der Promotion: 16. 05. 2010

Erklärung

Ich, Enhong, Zhong, erkläre, dass ich die vorgelegte Dissertationsschrift mit dem Thema: „Investigation of the transcriptional regulation and function of TFF1 in female reproductive organs“ selbst verfasst und keine anderen als die angegebenen Quellen und Hilfsmittel benutzt, ohne die unzulässige Hilfe Dritter verfasst und auch in Teilen keine Kopien anderer Arbeiten dargestellt habe.“

Datum

30 11 2009 (Nov 30, 2009)

A handwritten signature in black ink, reading "Enhong Zhong". The signature is written in a cursive, flowing style.

Unterschrift (Enhong Zhong)

1.	CHAPTER 1: INTRODUCTION	1
1.1.	TFF1 protein and gene	1
1.2.	Tissue distribution of TFF1 peptide	4
1.3.	Biological function of TFF1 peptide	7
1.4.	Transcriptional regulation of TFF1	10
1.4.1.	Transcriptional regulation by transcriptional factors	10
1.4.2.	Transcriptional regulation of TFF1 by estrogen through ER	13
1.4.2.1	Estrogen receptors	13
1.4.2.2.	Mechanisms through which ERs mediate the transcriptional regulation of target gene	14
1.4.2.3.	Transcriptional regulation of TFF1 by ERs	15
1.5.	Impact of TFFs on E-cadherin regulation	17
1.6.	Objectives	18
2.	CHAPTER 2: MATERIALS AND METHODS	20
2.1.	Materials	20
2.1.1.	Bacteria and plasmid	20
2.1.2.	Antibodies	20
2.1.3.	Chemicals	21
2.1.4.	Reagents	21
2.1.5.	Taqman probes	22
2.1.6.	Oligonucleotides	23
2.1.7.	Machines and instruments	23
2.2.	Methods	24
2.2.1.	Isolation of total RNA from cells and tissues	24
2.2.2.	Reverse transcription and polymerase chain reaction	25
2.2.3.	Quantitative real-time PCR analysis	27
2.2.3.1.	Construction of the target DNA plasmids	27
2.2.3.2.	Transformation of DNA plasmid into DH5α into competent cells	27
2.2.3.3.	Maxi preparation of DNA plasmid	28

2.2.3.4.	Quantitative real-time PCR analysis	29
2.2.4.	Western blot	30
2.2.4.1.	Total protein preparation from cells and tissues	30
2.2.4.2.	Quantitative analysis of protein content	31
2.2.4.3.	Western blot analysis	31
2.2.5.	Laser scan confocal microscopy and immunofluorescence analysis	32
2.2.6.	Transient transfection assays	33
2.2.7.	Luciferase and β -galactosidase assay	34
2.2.8.	Establishment of the <i>hTFF1-luc</i> transgenic rat model	34
2.2.8.1.	Construction of the <i>hTFF1</i> -pGL3 vector	34
2.2.8.2.	Transient transfection assays	35
2.2.8.3.	Generation of the <i>hTFF1-luc</i> transgenic rats	35
2.2.8.4.	Identification of the <i>hTFF1-luc</i> transgenic rat founders	36
2.2.8.5.	Generation of the <i>hTFF1-luc</i> heterozygous and homozygous transgenic rat lines	37
2.2.9.	Estrous cycle determination and sacrifice of the <i>hTFF1-luc</i> transgenic rats	37
2.2.10.	<i>In vivo</i> bioluminescent imaging	37
2.2.11.	RT-PCR to identify the tissue-specific expression of the luciferase transgene in the <i>hTFF1-luc</i> transgenic rats	39
2.2.12.	Luciferase enzyme activity assay in <i>hTFF1-luc</i> transgenic rats	39
2.2.13.	Hormonal analysis	40
2.2.14.	Estrous cycle determination and sacrifice of the TFF1 knock out mice	40
2.2.15.	Gross morphological and histological analysis of female reproductive organs in TFF1 knock out mice	41
2.2.16.	Measurement of the thickness of epithelial layer	41
2.2.17.	Electron microscopy analysis	41
2.2.18.	Statistical analysis	42
3.	CHAPTER 3: RESULTS	43

3.1.	Transcriptional regulation of TFF1 by E2 <i>in vitro</i>	43
3.1.1.	E2 was able to enhance the TFF1 transcription	43
3.1.2.	10 ⁻¹⁵ M estradiol upregulated the TFF1 expression, whereas 10 ⁻⁵ M estradiol downregulated its expression	44
3.1.3.	Estradiol, ICI 182 780 and tamoxifen regulated the TFF1 expression by downregulation of ER α expression in cytosol	45
3.1.4.	Estradiol, and ICI 182 780 downregulated ER α expression, but tamoxifen upregulated ER α expression in nucleus	47
3.1.5	TFF1 activated the E-cadherin promoter in the presence of estradiol	48
3.2.	<i>In vivo</i> experiments I	50
3.2.1.	Generation and identification of <i>hTFF1-luc</i> transgenic rats	50
3.2.1.1.	Establishment of the <i>hTFF1</i> -pGL3 construct	50
3.2.1.2.	<i>hTFF1-luc</i> transgenic rat lines	52
3.2.1.3.	<i>In vivo</i> bioluminescence imaging of the <i>hTFF1-luc</i> transgene in living animals	52
3.2.2.	Tissue expression fashion of luciferase transgene	55
3.2.2.1.	Luciferase transgene was highly expressed in brain, followed by heart, stomach, colon, uterus, vagina and ovary	55
3.2.2.2.	<i>In vitro</i> luciferase activity assay confirmed the highest luciferase activity in brain, not in vagina	56
3.2.3.	The luciferase transgene was localized in the vessel of the brain tissue	58
3.2.4.	The <i>hTFF1</i> promoter was activated by the serum estrogen during natural estrous cycle in <i>hTFF1-luc</i> ^{+/+} transgenic rats	59
3.2.4.1.	Generation and identification of the <i>hTFF1-luc</i> ^{+/+} transgenic rats	59
3.2.4.2.	Luciferase activity was significantly increased in the tissues from the female <i>hTFF1-luc</i> ^{+/+} rats at proestrous stage	61

3.2.4.3.	Luciferase mRNA increased in the tissues from <i>hTFF1-luc^{+/+}</i> rats at proestrous than that at estrous and diestrous stages	65
3.2.4.4.	Luciferase protein was upregulated in the tissues from the <i>hTFF1-luc^{+/+}</i> rats at the proestrous stage	66
3.3.	<i>In vivo</i> experiments II	69
3.3.1.	Characterization of the TFF1 knock out mice	69
3.3.2.	Morphological alteration of uterus and vagina in the female TFF1 knock out mice	70
3.3.2.1.	Loss of TFF1 led to uterine hyperplasia	70
3.3.2.2.	Loss of TFF1 led to increased thickness of total uterine and vaginal epithelial layer	73
3.3.2.3.	Loss of TFF1 led to loss of cell-cell contact and cell-cell adhesion in the uterine and vaginal epithelium	79
3.3.2.4.	Loss of TFF1 led to downregulation of E-cadherin but not β -catenin expression in the uterus and vagina	81
3.3.2.5.	Loss of TFF1 was unable to trigger the translocation of E-cadherin and β -catenin from epithelial cell membrane to cytoplasm or nucleus	85
3.3.2.6.	Loss of TFF1 led to increased expression of ER α but not ER β in the uterus	88
3.3.2.7.	Loss of TFF1 might result in increased ER α expression in the vagina from TFF1 knock out mice at diestrous stage.	90
4.	CHAPTER 4: DISCUSSION	91
4.1.	Transcriptional regulation of TFF1 by estradiol <i>in vitro</i>	91
4.1.1.	The effect of estradiol, ICI 182 780 and tamoxifen on the TFF1 transcription and translation	91
4.1.2.	The effect of E2, ICI 182 780 and tamoxifen on the ER α expression	93
4.1.3.	Molecular mechanisms underlying the TFF1 transcriptional regulation by E2, ICI 182 780 and tamoxifen	94
4.1.4.	Mechanisms underlying the chromatin remodeling of TFF1 by estradiol	96
4.2.	Transcriptional regulation of TFF1 by estradiol <i>in vivo</i>	97

4.2.1.	Comparison of the advantages and disadvantages between GFP and luciferase reporter genes in transgenic model	97
4.2.2.	Tissue specific expression fashion of luciferase directed by hTFF1 promoter	98
4.2.3.	Possible mechanisms underlying the luciferase tissue specific expression directed by hTFF1 promoter	100
4.2.4.	The activation of the hTFF1 promoter in brain and the role of TFF1 in the vessel	103
4.2.5.	The activation of the hTFF1 promoter by physiological estrogen during the course of the estrous cycle	104
4.2.6.	The mechanisms underlying the transcriptional regulation of TFF1 by estrogen	105
4.3.	Biological function of TFF1 in the female reproductive organs	108
4.3.1.	The biological functions of TFF1 in the uterus and vagina	108
4.3.2.	The impact of loss of TFF1 on the E-cadherin expression	111
4.3.3.	Mechanisms underlying the interaction between TFF1 and E-cadherin	113
4.3.4.	Mechanisms underlying loss of TFF1 leading to uterine and vaginal hyperplasia	114
4.3.5.	Proposed mechanisms underlying loss of TFF1 results in the impaired reproductive capacity in the female mice	119
5.	CHAPTER 5: SUMMARY	121
6.	REFERENCE LIST	124
7.	ABBREVIATIONS	142
8.	CURRICULUM VITAE	144
9.	PUBLICATIONS	146
10.	ACKNOWLEDGEMENTS	149

CHAPTER 1: INTRODUCTION

1. 1. TFF1 protein and gene

Trefoil factor1 (TFF1, previously pS2) (Masiakowski et al., 1982), is originally identified as an estrogen-responsive gene in the MCF-7 human breast cancer cell line (Jakowlew et al., 1984), and belongs to the family of small regulatory proteins consisting of three mammalian members. The other two members are spasmodic polypeptide, TFF2 (SP) (Beck et al., 1996), and intestinal trefoil factor, TFF3 (ITF) (Schmitt et al., 1996). All the trefoil peptides have seven conserved cysteine residues, six of which form three intrachain disulfide bonds associating cysteines 1 and 5, 2 and 4, 3 and 6, that results in a characteristic three-loop structure named trefoil domain or P-domain (Fig.1), and thus, the trefoil factor family was given its name (Polshakov et al., 1997). TFF1 and TFF3 have one trefoil domain, whereas TFF2 has two trefoil domains.

The trefoil domain, which has been well conserved throughout evolution from amphibia to mammals, is extendedly defined as a conserved sequence of 42 or 43 amino acid residues. This trefoil domain renders the protein resistant to proteases and acid degradation (Suemori et al., 1991). Several molecular forms of TFF peptides have been identified as monomers, homodimers and heterodimers. The dimers are formed via intermolecular disulfide bonds between the seventh cysteine residue at the carboxyl terminus of the peptides, and are suspected of being more active and potent than monomers in a wounding model of restitution and stimulating migration of MCF-7 cells (Marchbank et al., 1998; Prest et al., 2002).

The genes encoding TFF peptides are located in a head to tail orientation, clustered in a 55 kb region on chromosome 21q22.3 (Fig. 2). It is demonstrated that in the position between the -428 to -332 5' flanking sequence of the TFF1 gene contains DNA enhancer elements responsive to estrogens, tumour promoter 12-O-tetradecanoylphorbol-13-acetate (TPA, which activates protein kinases C), epidermal growth factor (EGF), the c-Ha-ras oncoprotein (an oncoprotein corresponding

to a GTP-binding protein) and the c-jun protein (a putative proto-oncoprotein related to the trans-acting factor AP) (Nunez et al., 1989). The TFF1 5' flanking region also contains a TATA box, a CAAT box, AP1-like motif and a single imperfect estrogen responsive element (ERE) (Fig. 2) (Nunez et al., 1989).

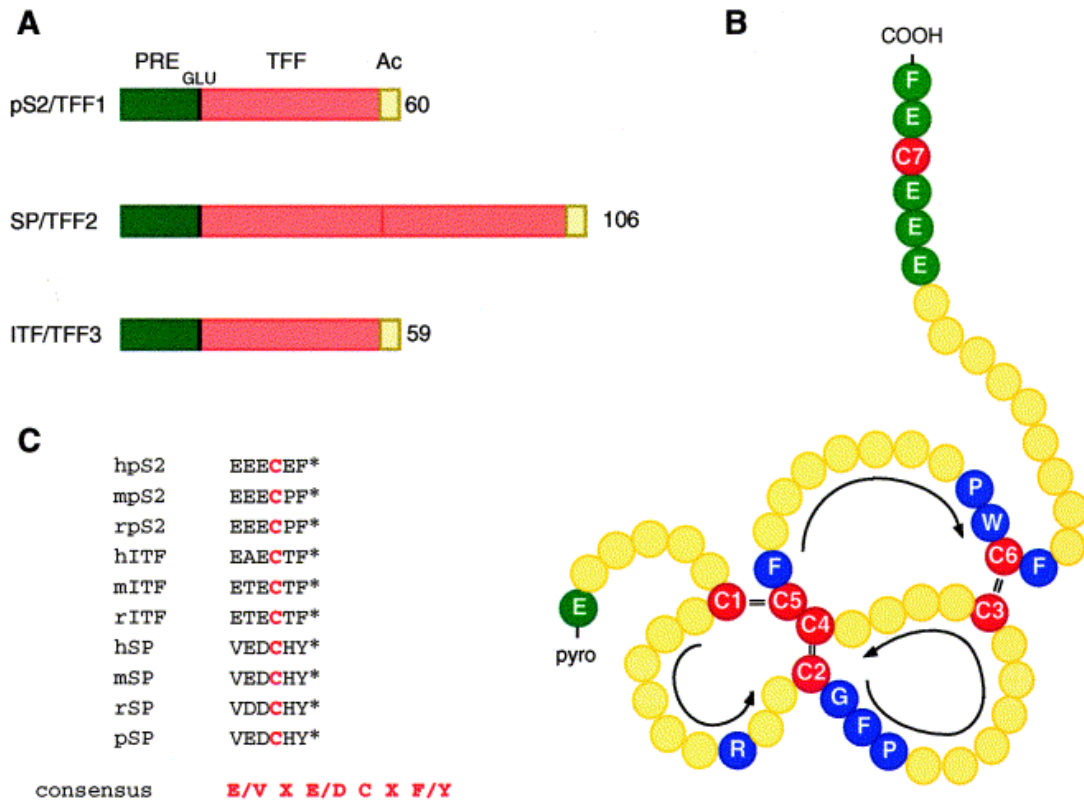


FIG.1. TFF1 protein structures

(A) Conserved primary protein structure of the three human TFFs, including a signal peptide (PRE; green), one or two TFF domains (TFF; red) and a carboxy-terminal acidic domain (Ac; yellow). GLU: glutamic acid. Numbers indicate the size of the mature proteins in residues. **(B)** Trefoil two dimensional structure. The one letter code is used, and only conserved amino acids are indicated. C1–C6 and the blue amino acids (AAs) represent the conserved AA of the TFF domain. C7 and the green AAs represent the Ac domain. = indicates the disulfide bonds between C residues. Arrows indicate the three loops resembling a clover-leaf. **(C)** Primary sequence conservation of the acidic domain in all mammalian TFFs. * indicates carboxy-terminal end of proteins. C: Cysteine; h, human; m, mouse; r, rat; p, pig (Ribieras et al., 1998)

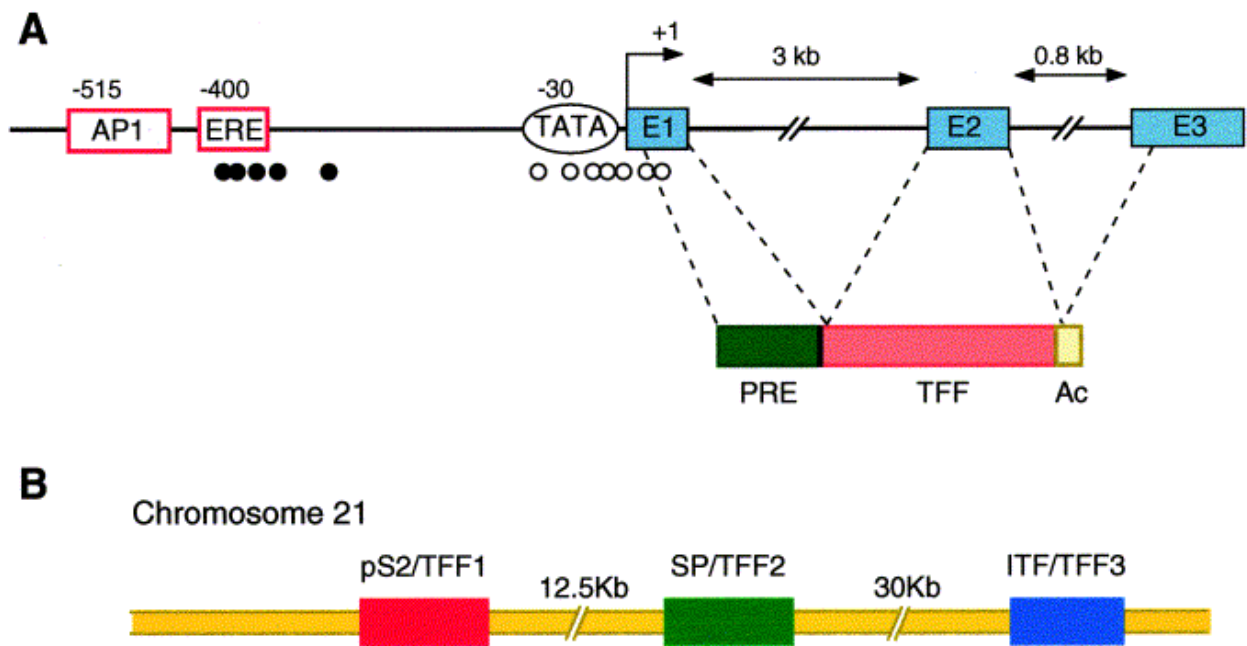


FIG. 2. TFFs gene structures

(A) Gene organization and regulatory elements. ERE: estrogen responsive element; AP1: jun/fos responsive element; TATA: TATA box; +1: start site of the transcription; exons are in blue; circles: CpG islands located at positions -420 to $+20$; black circles: CpG whose methylation is correlated with TFF1 expression; a signal peptide (PRE; in green); TFF domains (TFF; in red) and a carboxy-terminal acidic domain (Ac; in yellow). **(B)** TFFs cluster on the human chromosome 21. Kb: kilobases (Ribieras et al., 1998)

Transient transfection assays have demonstrated that the single imperfect ERE confers estrogen responsiveness (Nunez et al., 1989). The ERE of the TFF1 gene has been narrowed down by site-directed deletion mutagenesis to a 13-base-pair (position -405 to position -393) imperfectly palindromic sequence 5'-GGTCACGGTGGCC-3' (Fig. 3) (Berry et al., 1989), and differing by 1 bp in its 3' stem from the canonical perfect palindromic ERE (5'-GGTCANNNTGACC-3'), which is present in the *Xenopus laevis* vitellogenin A2 gene, is an inverted palindromic sequence separated by three intervening nucleotides (Klein-Hitpass et al., 1988). Deletion of the TFF1 ERE abolishes estrogen response, but not TPA, c-Ha-ras, c-jun or EGF responses (Nunez et al., 1989).

membranes of Golgi apparatus and surface/pit gastric mucous cells (Sarraf et al., 1995). TFF peptides are often co-secreted with mucins into the lumen to form a gel-like mucus layer. Accordingly, TFF1 interacts with MUC5AC through binding to the von Willebrand factor C cysteine-rich domains VWFC1 and VWFC2 (Tomasetto et al., 2000), whereas TFF2 is co-localized with MUC6 and TFF3 is co-localized with MUC2 (Tab. 1) (Longman et al., 2000). It is through association with mucins that TFF peptides influence protection and healing of the gastrointestinal mucosa, serving as a barrier to protect the epithelium from mechanical stress, noxious agents, viruses, and other pathogens.

Table 1. TFF peptides synthesized in the normal human gastrointestinal tract

Organs	Cell	TFF peptide	Secretory Mucin
Salivary glands	Submandibular glands	TFF3	MUC7 or MUC5B
Esophagus Stomach	Minor salivary glands	TFF3	MUC5B
	Submucosal glands	TFF3	MUC5B
	Cardiac SMCs	TFF1, TFF3	MUC5AC
	Corpus SMCs	TFF1	MUC5AC
	Antral SMCs	TFF1, TFF3	MUC5AC
Intestine	MNCs	TFF2	MUC6
	Antral glands	TFF2	MUC6
	Brunner's glands	TFF2, TFF3	MUC2
Vater's ampulla Pancreas	Goblet cells	TFF3	MUC5AC/B, MUC6 (MUC6)
	Goblet cells (Duct epithelium), islets	TFF3 (TFF1), TFF3	
Liver	LBDs, SBDs, PBGs	TFF1, (TFF2), TFF3	MUC6
Gallbladder	Epithelial cells	(TFF1), (TFF2), TFF3	(MUC5B), MUC6

Scarce TFF peptide levels are indicated by parentheses. Also shown are the secretory mucins, often co-expressed. SMC, surface mucous cell; MNC, mucous neck cell; LBD, large biliary duct; SBD, small biliary duct; PBG, peribiliary gland (Hoffmann, 2006).

Besides their expression in the gastrointestinal system, TFF1 and TFF3 are also detected in salivary glands, corneal, conjunctival, and lymphoid tissues where they might play a role in inflammation and epithelial ulceration (Emami et al., 2004). The presence of TFF1

and TFF3 in human hypothalamus, pituitary, gastric juice, and urine is also demonstrated, suggesting the paracrine, autocrine and endocrine functions for these peptides (Hoffmann and Jagla, 2002).

In addition, TFF1 is also described in tissues such as heart, spleen, muscle and brain in the adult mouse (Hirota et al., 1994). It is demonstrated that the TFF1 mRNA was additionally detected in astrocytes cultured from the whole brain of the newborn mouse, where it reached its maximal level at day 3 after birth, and then gradually decreased after confluence had been reached. Therefore, TFF1 mRNA is considered to be correlated with the growth of mouse astrocytes. Furthermore, it was shown that the TFF1 mRNA was especially expressed in the late G1/S phase of the cell cycle in astrocytes (Hirota et al., 1994). In the adult rat brain, TFF1 mRNA was predominantly expressed in hippocampus, followed by the cerebral cortex and cerebellum. The developmental expression of TFF1 mRNA in hippocampus, which is known to mature after birth, showed a clear peak in 1- or 3-day-old rats, and gradually decreased by 7 weeks after birth. In midbrain, the maturation of which occurs at an early developmental stage, TFF1 mRNA was retained at a low level from postnatal 1 day to week 7. Summarizing those data leads to the hypothesis that TFF1 protein plays an important role in the development of the central nervous system (Hirota et al., 1995).

In mouse embryos, from 8 day post coitum to birth, TFF1 is only observed in the developing stomach, all other tissues studied being negative (Lefebvre et al., 1993). At day 17, TFF1 starts to express in the epithelial cells lining the surface and the nascent stomach pits and glands (Lefebvre et al., 1993). In addition, 18 day embryos show expression of both TFF1 and TFF2 in the glands of the gastro-duodenal junction corresponding to the developing Brunner's glands. Although TFF2 continues to express in Brunner's glands, TFF1 is not observed there beyond post-natal day 14 (Lefebvre et al., 1993). TFF3 is not expressed during embryonic development. It first becomes detectable in 3-day-old mice (Mashimo et al., 1996).

In addition, TFF1 is demonstrated to be expressed in the human and mouse uterus and vagina as well (Wiede et al., 2001; Masui et al., 2006; Lefebvre et al., 1993; Rye et al., 1993). It is demonstrated that vaginal expression of TFF1 mRNA is markedly increased by estrogens in neonatal mice but not in adults, and its expression is even observed when the neonatally estrogenized mice come into adulthood (Masui et al., 2006).

Furthermore, under pathological circumstances, TFF1 is shown to be ectopically expressed in gastrointestinal inflammatory disorders such as Crohn's disease, duodenal peptic ulcer, hemorrhagic rectocolitis (Rio et al., 1991; Wright et al., 1990; Rio and Chambon, 1990), and in various human solid tumors of the mammary gland, pancreas, large bowel, biliary tract, lung, esophagus, bladder, prostate and mucinous-subtype ovarian as well as in their associated metastases (Ribieras et al., 1998).

1. 3. Biological functions of TFF1 peptide

The biological functions of TFF1 are not very well understood, especially, in the female reproductive system. Most studies are mainly related to the gastrointestinal tract. It is demonstrated that TFF1 plays a crucial role in mucosal defense and healing. In case of mucosa aggression (due to bacteria, virus or medication), inflammatory diseases and ulcerous pathology, TFF1 is involved in epithelium regeneration, mucus stabilization and stimulation of normal epithelial cells restitution during wound repair in the stomach (Mathelin et al., 2005; Emami et al., 2004). In wound healing assays, TFF1 is up-regulated during gastrointestinal damage as motogens to induce cell migration in gastrointestinal epithelial cells to protect the mucosa in the gastrointestinal tract (Emami et al., 2004). Ectopic overexpression of TFF1 in the rat jejunum, using the intestinal fatty acid-binding protein promoter (pFABP), protects the mucosa from drug-induced damage (Playford et al., 1996). Furthermore, it is reported that TFF1 is involved in the differentiation of epithelial cells and leads in a TFF1 knock-out mouse model to improper differentiation and dysfunction of stomach and small intestine (Lefebvre et al., 1996). Indeed, it is shown that TFF1 participates in gastrointestinal cell differentiation by delaying G1-S phase transition and reducing apoptosis (Bossenmeyer-Pourie et al.,

2002). In addition, TFF1 is required and controls the commitment program of epithelial progenitors in the mouse oxyntic mucosa (Karam et al., 2004). Moreover, TFF1 peptide is considered as the early embryonic marker of epithelial cell differentiation in rat intestine and stomach (Familarì et al., 1998) due to its expression at day 17 in the epithelial cells lining the surface, the nascent stomach pits and glands of mouse embryos (Lefebvre et al., 1993).

TFF1 functions as a gastric tumor suppressor gene under physiological conditions and is involved in the neoplastic progression of the digestive system with the other TFFs (Prest et al., 2002; Rodrigues et al., 2001). Interference with cellular attachment has been implicated during the neoplastic process (Pignatelli and Vessey, 1994), in which there is a disruption of tissue architecture and a derangement in differentiation in tissue. It is demonstrated that in a TFF1 knock-out mouse model, the antral and pyloric gastric mucosa is dysfunctional and exhibits severe hyperplasia and dysplasia, and the development of adenoma and carcinoma in the stomach (Lefebvre et al., 1996). Downregulation of human TFF1 levels through hypermethylation of the TFF1 promoter seems to be implicated in tumor formation at early stages of gastric carcinogenesis (Fujimoto et al., 2000). In support of a tumor suppressor role, both TFF1 and TFF3 are demonstrated to reduce the growth of the human colon cancer cell lines LoVo and SW837 *in vitro* and *in vivo*, which is accompanied by reduced mitogen activated protein kinase (MAPK/ERK) phosphorylation and activation (Calnan et al., 1999). Furthermore, TFF1 shows the ability to lower gastrointestinal cell proliferation by delaying the G1-S phase transition, and increases the levels of the cyclin-dependent kinase inhibitors p16INK4 and p21CIP1/Waf1. Both p21Cip1/Waf1 and p16INK4 inhibit the activity of cyclin D1/cdk4 and cyclin E/cdk2 complexes, which phosphorylate and inactivate the retinoblastinoma tumor suppressor pRb1. This leads to the sequestration of the transcription factor E2F involved in the expression of a large panel of genes essential for cell cycle progression and DNA replication (Bossenmeyer-Pourie et al., 2002).

However, under pathological conditions, TFF peptides function as tumor progression factors and proangiogenic factor and promote tumor cell invasion (Prest et al., 2002; Rodrigues et al., 2001). Evidence of TFF1 overexpression has been found in a range of carcinomas such as breast, bowel, prostate, pancreas, thyroid and lung carcinomas (Ribieras et al., 1998). In some breast cancers, TFF1 is overexpressed independently of the estrogen receptor (ER) status, even though estrogen induces cancer cell migration and the formation of complex branched structures, probably through TFF1 (Crosier et al., 2001; Lalani et al., 1999; Prest et al., 2002). Some studies show that TFF peptides are involved in cell scattering and tumor cell invasion via autocrine and paracrine loops (Rodrigues et al., 2001; Emami et al., 2001). Exogenous TFF peptides alone are not sufficient to induce the invasive phenotype in premalignant human colonic adenoma cells PC/AA/C1 and kidney MDCK epithelial cells, but require the priming and permissive action of src and RhoA to exert their proinvasive activity, as shown in their src- and RhoA-transformed counterparts (Emami et al., 2001). Conversely, ectopic expression of TFF1 is sufficient to induce a constitutive invasive phenotype in stably transfected human colorectal cancer cells HCT-8/S11-TFF1 through a RhoA-independent mechanism. In addition, it has recently shown that TFF peptides function as proangiogenic factors through cyclooxygenase-2 and EGF receptor signaling *in vivo* and *in vitro* (Rodrigues et al., 2003) .

An antiapoptotic role is also proposed for TFFs. TFF1 protects cells from anoikis (an anchorage-dependent form of apoptosis induced by cell detachment from the substratum), chemical-, or Bad-induced apoptosis, by reducing caspase-3, caspase-6, caspase-8, and caspase-9 activities (Bossenmeyer-Pourie et al., 2002). It has been observed that TFF2 reduces apoptosis induced by serum starvation and anoikis by decreasing the number of apoptotic bodies and DNA fragmentation in the breast cancer cell line MCF-7 (Lalani et al., 1999). Cell lines overexpressing TFF3 are resistant to serum starvation and drug-induced apoptosis (Kinoshita et al., 2000; Taupin et al., 2000). Mice deficient in TFF3 show increased apoptosis in colon cells, unaccompanied by changes in expression of receptor-related (TNFR/Fas) or stress-related (Bcl-family) cell

death regulators (Taupin et al., 2000). TFF3 also blocks apoptosis in a p53-dependent manner after challenge with the topoisomerase inhibitor etoposide in human colonic cancer cells HCT116 and in the non-transformed rat intestinal epithelial cell line IEC-6.

TFF peptides exert their action not only extracellularly but also are considered to contribute to protein folding within the cells. The lack of TFF1 leads to an accumulation of misfolded proteins in the endoplasmic reticulum. Consequently, several abnormal proteins, including GRP78, ERp72, p58IPK CHOP10, and clusterin, are accumulated in the endoplasmic reticulum machinery in TFF1 knock-out antropyloric tumors (Torres et al., 2002).

Nevertheless, the biological functions of TFF1 in female reproductive organs are not well understood. It is considered that TFF1 might play a major role while influencing the rheological properties of the endocervical mucus (Wiede et al., 2001). But whether and how TFF1 influences differentiation of epithelial cells in the female reproductive system is still unknown.

1. 4. Transcriptional regulation of TFF1

1. 4. 1. Transcriptional regulation by transcriptional factors

The human TFF1 gene is about 4.5 kb long and consists of three exons (Fig. 2). The proximal 5' flanking region contains typical regulatory elements like a TATA box, a CACT element, and a GC rich motif (Nunez et al., 1989d). Further upstream, a functional AP-1 like site between -518 and -512 (Gillesby et al., 1997), a single imperfect ERE between -405 and -393, and a complex enhancer region responsive to EGF, the tumor promoter TPA and the protooncoproteins c-Ha-ras and c-jun are detected between -428 and -332. The ERE and the TATA box are each located at the edge of a nucleosome. Furthermore, motif II (adjacent to the ERE and considerably matching the binding site of heat shock factor HSH-2) and motif III (close to the TATA box matching a GATA consensus sequence) are discovered due to their similarity to sequences in the 5' flanking region of TFF2 (Beck et al., 1998; Gott et al., 1996). Therefore, the cell-specific expression of the TFF1 gene is

coordinately regulated by several transcription factors, regulatory proteins and epigenetic factors such as estrogens, EGF, gastrin, FGF2/bFGF, FGF7/KGF, upstream stimulating factor (USF), hepatocyte nuclear factor-3, GATA-6, and Ha-Ras/AP-1 by binding to their corresponding binding sites in the promoter (Nunez et al., 1989; Miyashita et al., 1994; Khan et al., 2003).

It is demonstrated that 17 β -estradiol (E_2) is able to regulate the transcription of the single-copy TFF1 gene and results in increased levels of TFF1 mRNA and secreted protein (Brown et al., 1984).

EGF is proposed to regulate the expression of TFF1 in stomach at the post-transcriptional level (Miyashita et al., 1994), since EGF is known to have an effect on the stomach where it inhibits acid secretion (Carpenter and Cohen, 1979). Thus, the EGF-responsive element in the TFF1 promoter region may control expression of the TFF1 gene, which may be one of the EGF target genes in the stomach (Nunez et al., 1989f). It is further suggested that there are also complex synergistic effects with EGF and TPA, which is suggested to induce the translation of TFF1 mRNA but not in its transcription. Therefore, It has been suggested that in the gastrointestinal tract, TFF1 expression could be estrogen-independent but EGF-dependent (Ribieras et al., 1998). In addition, it is reported that the gastric hormone gastrin is a well-defined positive regulator of TFF1 in the stomach. Khan et al (Khan et al., 2003) have identified a gastrin responsive element in the human TFF1 promoter, and have shown that both human and mouse TFF1 gene can be activated by this hormone in the stomach. Regulatory sequences responsible for stomach-specific expression of TFF1 are probably motif II and motif III (Beck et al., 1998b). The latter is identified as a GATA-6-binding sequence that activates gastric expression probably together with additional GATA sites at -174, -124, and -110 (Al-azzeah et al., 2000; Al-azzeah et al., 2000). HNF-3 specifically activates TFF1 via motif IV, which is probably of importance during inflammatory conditions and neoplasia (Beck et al., 1999).

The putative GATA-binding site, located 32 bp upstream of the TATA box (AGATAA) is conserved in its flanking sequences and position between the two stomach-specific

genes TFF1 and TFF2. The GATA-6 transcription factor was shown to express in a variety of gastric, intestinal, and pancreatic tumor cell lines. Cotransfection with GATA-6 expression vectors and TFF reporter genes revealed that GATA-6 activates TFF1 and TFF2 4-6-fold without an effect on TFF3 (Al-azzeah et al., 2000).

Furthermore, in gastric cell lines low micromolar concentration of TFFs can stimulate their own as well as other family members' release. And both TFF2 and TFF3 can up-regulate the transcription of TFF1 and TFF2 (Bulitta et al., 2002) by binding to cis-regulatory elements of their respective promoters in a mitogen-activated protein kinase-(MAPK/Erk)-dependent fashion (Taupin et al., 1999). Cross-induction of trefoils requires indirect activation of the EGF receptor since both TFF2- and TFF3-induced trefoil expression is dependent on EGF receptor phosphorylation (Taupin et al., 1999).

The inflammatory cytokines interleukin (IL)-1 β and particularly IL-6 are important regulators of trefoil gene expression. It is reported that both IL-1 β and IL-6 can repress TFF1 promoter activity and gene expression synergistically via inhibition of nuclear factor (NF- κ B) and CCAAT enhancer-binding protein (C/EBP), respectively (Dossinger et al., 2002). Furthermore, a repression of TFF1 expression is observed by retinoic acid (Hirota et al., 1992).

Additional regulation by several growth factors, such as insulin, insulin-like growth factor I (IGF-I), basic fibroblast growth factor (bFGF), and X-ray irradiation, phorbol ester TPA/protein kinase C (PKC), aspirin, arachidonic acid, PPAR γ ligands, and hydrogen peroxide are involved in trefoil peptide gene expression (Azarschab et al., 2001; Balcer-Kubiczek et al., 2002; Shimada et al., 2003). Enteric neurotransmitters, acetylcholine, TNF α , short-chain fatty acids, and glucose, all regulate TFF peptides expression and secretion (Loncar et al., 2003; Moro et al., 2001; Ogata and Podolsky, 1997; Taupin and Podolsky, 1999; Tebbutt et al., 2002; Tran et al., 1998)

In addition, methylation of the TFF1 promoter was shown to play an important role in its transcription and tissue expression. It has been reported that the TFF1 gene exhibits

tissue-specific methylation of its proximal promoter/enhancer region that correlates with its expression. Specific sequences are methylated in non-expressing tissues and cell lines but unmethylated in those which express TFF1 (Martin et al., 1995; Martin et al., 1997). But the methylation status of the TFF1 promoter region changes in different tumors and clearly affects TFF1 expression. For example, the region around the ERE is hypomethylated in ER-rich breast tumors, which causes ectopic TFF1 expression. Surprisingly, the ERE is not only recognized by the ER but also by a methylation-sensitive DNA-binding protein. In contrast, hypermethylation of CpG sites within the TFF1 promoter region is observed at an early stage of stomach carcinogenesis resulting in reduced TFF1 expression (Hoffmann and Jagla, 2002).

1. 4. 2. transcriptional regulation of TFF1 by estrogen through ER

The human TFF1 gene is initially characterized as a gene whose expression is specifically controlled by estrogen in the breast cancer cell line MCF-7 (Jakowlew et al., 1984). It is demonstrated that exposure of MCF-7 human breast cancer cells to E₂ activates transcription of the single-copy TFF1 gene and results in increased levels of TFF1 mRNA and secreted protein (Brown et al., 1984). Regulation of TFF1 expression by estrogen requires the presences of ERs, which explains why expression of TFF1 is restricted to a subclass of ER-rich human breast tumors.

1. 4. 2 .1. Estrogen receptors

More than 30 years ago, Jensen and Jacobsen (Jensen and Jacobsen et al., 1962) came to the conclusion, based on the specific binding of estrogen in the uterus, that the biological effects of estrogen have to be mediated by a intracellular receptor protein, and in 1986, the cloning of this ER was reported (Greene et al., 1986). And in 1995, a second ER, ER β , was cloned from a rat prostate cDNA library (Kuiper et al., 1996). The former ER is now called ER α . Both ER α and ER β belong to the steroid/thyroid hormone superfamily of nuclear receptors, members of which share a common structural architecture (Giguere et al., 1988). They are composed of three independent but

interacting functional domains: the NH₂-terminal or A/B domain, the C or DNA-binding domain, and the D/E/F or ligand-binding domain. Binding of a ligand to ER triggers conformational changes in the receptor and this leads, via a number of events, to changes in the rate of transcription of estrogen-regulated genes. These events, and the order in which they occur in the overall process, are not completely understood, but they include receptor dimerization, receptor-DNA interaction, recruitment and interaction with coactivators and other transcription factors, and formation of a preinitiation complex (Beekman et al., 1993; Katzenellenbogen and Katzenellenbogen, 1996; Kraus and Kadonaga, 1998; Kraus et al., 1995; Shibata et al., 1997).

The N-terminal domain of ERs encodes a ligand-independent activation function (AF1) (McInerney and Katzenellenbogen, 1996), a region of the receptor involved in protein-protein interactions (Onate et al., 1998), and transcriptional activation of target-gene expression. The DNA binding domain (DBD) contains a two zinc finger structure, which plays an important role in receptor dimerization and in binding of receptors to specific DNA sequences (Schwabe et al., 1993). ER α and ER β can be expected to bind to various EREs with similar specificity and affinity. The COOH-terminal, E/F-, or ligand-binding domain (LBD) mediates ligand binding, receptor dimerization, nuclear translocation, and transactivation of target gene expression (Tsai and O'Malley, 1994). The LBD also harbors activation function 2 (AF2), which is a complex region whose structure and function are governed by the binding of ligands (Henttu et al., 1997).

1. 4. 2. 2. Mechanisms through which ERs mediate the transcriptional regulation of target genes

For several years it was thought that the only mechanism through which estrogens affected transcription of estrogen sensitive genes was by direct binding of the activated ER to an EREs. These EREs were first observed in the 5'-flanking region of the *Xenopus vitellogenin A2* gene (Klein-Hitpass et al., 1986). Today we know that ER α and ER β can also modulate the expression of genes without directly binding to DNA (Fig. 4). One example is the interaction between ER α and the c-rel subunit of the NF κ B complex. This

interaction prevents NF κ B from binding to and stimulating expression from the interleukin-6 (IL-6) promoter (Galien and Garcia, 1997). In this way, E₂ inhibits expression of the cytokine IL-6 (Galien and Garcia, 1997). Another example of indirect action on DNA is the physical interaction of ER α with the Sp1 transcription factor (Porter et al., 1997). ER α enhancement of Sp1 DNA binding is hormone-independent (Porter et al., 1997), and both ER α and ER β can activate transcription of the retinoic acid receptor α 1 (RAR-1) gene, presumably by the formation of an ER-Sp1 complex on GC-rich Sp1 sites in the RAR1 promoter (Sun et al., 1998). Besides, both ER α and ER β can interact with the fos/jun transcription factor complex on AP1 sites to stimulate gene expression, however, with opposite effects in the presence of estrogen (Paech et al., 1997; Webb et al., 1999).

1. 4. 2 .3. Transcriptional regulation of TFF1 by ERs

It was demonstrated that E₂ is able to activate the transcription of a single-copy TFF1 gene resulting in increased levels of TFF1 mRNA and secreted protein in MCF-7 human breast cancer cells (Brown et al., 1984). Regulation of TFF1 expression by estrogen requires the presences of ERs. It was demonstrated that ERs are able to induce the high levels of transcription of TFF1 (Giamarchi et al., 2002; Surowiak et al., 2001). ER α has a higher affinity and is a more potent activator of transcription of TFF1 than ER β . In ER-rich human breast tumors, the ERE is clearly the predominant element directly controlling the TFF1 transcription. Therefore, the transcriptional regulation of TFF1 by estrogen seems to function through the classic ERE model. Estrogens exert their transcriptional regulation effects on the target gene by binding to the different ERs in the cytoplasm (Nilsson et al., 2001). Binding of estrogens, such as E₂, or ethinyl-17- β -estradiol (EE₂), to the ERs induces dissociation of heat shock protein-chaperone complex (HSP90) from ERs, which enables the ERs to dimerize and to enter the nucleus where the ER complex binds to EREs within the TFF1 promoter (Fig.5). After binding to the ligand of estrogen, the ER ligand binding domain (LBD) assumes a conformation that enables the recruitment of coactivators, proteins which help to assemble a multiprotein complex that facilitates both chromatin remodeling and formation of an active transcription complex (Aranda and Pascual, 2001; McEwan, 2000; McKenna et al., 1999).

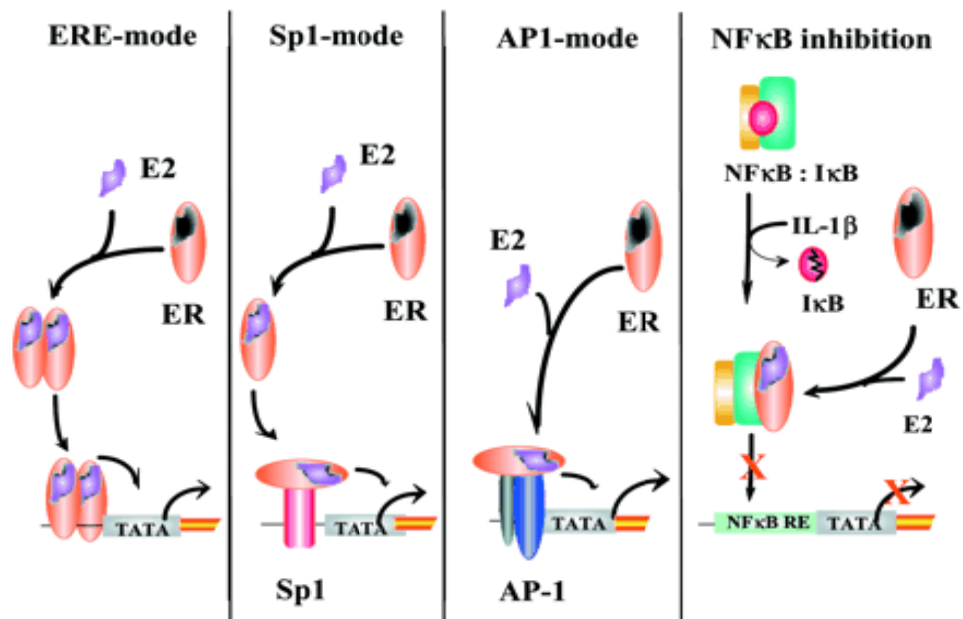


FIG.4. Model representing the various modes through which ERs can modulate transcription of genes

In the first panel is depicted the classical interaction of the activated receptor with EREs on DNA. In the other three panels are representations of the indirect effects of ERs on transcription interactions. This occurs through protein-protein interactions with the Sp1, AP1, and NF κ B proteins (Nilsson et al., 2001).

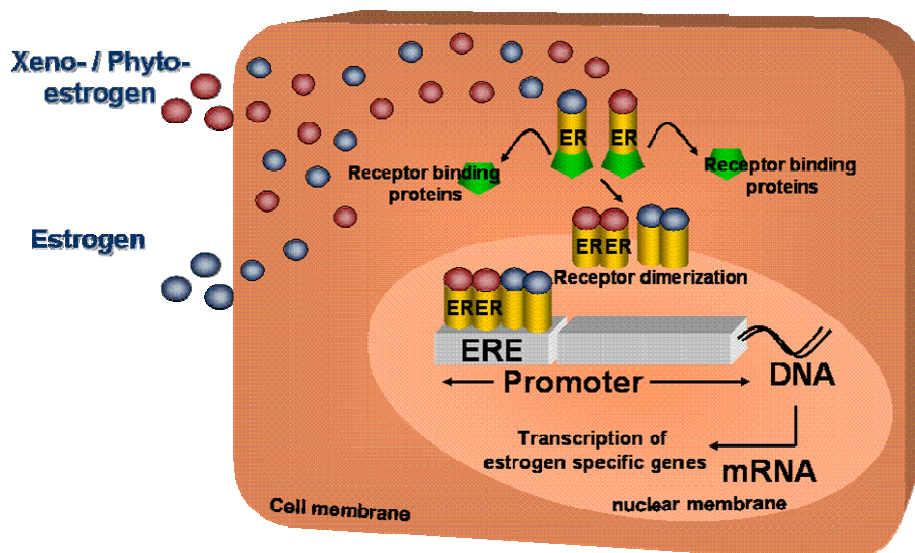


FIG. 5. Proposed mechanism through which estrogen activates transcriptional regulation of target genes such as TFF1 (Schonfelder G)

The EREs sequences normally are protected by proteins in the ER-containing nuclear extracts (Wood et al., 2001). But the extent of the protection is dependent on the sequence of the EREs. In the TFF1 promoter, the two ERE half-sites are minimally protected (Wood et al., 2001). Interestingly, protease sensitivity assays demonstrate that different EREs induce distinct changes in ER α and ER β conformation thereby providing different functional surfaces for interaction with regulatory proteins involved in control of estrogen-responsive genes. In contrast, it is also shown that ERs are able to induce conformational changes in DNA fragments containing the *Xenopus laevis* vitellogenin A2 and imperfect EREs (Nardulli et al., 1996; Nardulli et al., 1993). These ER-induced changes in DNA structure could increase the accessibility of sequences flanking the ERE to DNase I cleavage. DNase I and dimethyl sulfate (DMS) *in vivo* footprinting analysis revealed that in MCF-7 cells, unoccupied ER is bound to the consensus ERE half site in the absence of hormone and that an estrogen-occupied ER is bound to both ERE half sites in the presence of hormone (Kim et al., 2000). Thus, estrogens can induce TFF1 gene expression in hormone-dependent breast cancer cells, and act synergistically with the steroid receptor coactivator-1 (SRC-1) via the activator protein 1 (AP1) on the EREs presented in the TFF1 promoter (Barkhem et al., 2002b; Barkhem et al., 2002a). The AP1 site located at -332 to -338 within the TFF1 promoter has a dominant role in the response to estrogens. The potentiation of TFF1 promoter activity by the AP1 motif in response to estrogen is dependent on the ligand binding domain of ER α as well (Barkhem et al., 2002a). It is proposed that binding of ER α and activation of the ERE by estrogen in the TFF1 promoter is augmented in the presence of intact Sp1 and Sp3 binding sites by regulating the histone acetylation (Sun et al., 2005).

1. 5. Impact of TFFs on E-cadherin regulation

E-cadherin, a 120-KDa transmembrane glycoprotein localized at the adherens junctions, is primarily responsible for the mediation of cell-cell adhesion in epithelial cells (Takeichi, 1991). In the presence of Ca²⁺, E-cadherin's extracellular domain interacts homotypically with the E-cadherin's molecules of neighboring cells to maintain intercellular adhesion,

and its cytoplasmic carboxy tail associates with a group of closely related but distinct membrane undercoat proteins, termed the catenins (α , β , and γ) (Gumbiner and McCrea, 1993). Both β -catenin and γ -catenin bind directly to the cytoplasmic domain of E-cadherin, and α -catenin links the β - and γ -catenin to the actin microfilament network of the cellular cytoskeleton (Nieset et al., 1997). Such binding is essential for the adhesive function of E-cadherin and for the establishment of tight physical cell-cell adhesion (Shimoyama et al., 1992).

It is demonstrated that the roles of TFF3 have been further linked to epithelial (E)-cadherin/catenin complexes that are the common targets for motogenic factors during cell migration. It is reported that TFF3 treatment is able to modulate the E-cadherin-catenin adhesion system in HT29 cells, leading to reduced E-cadherin, α -catenin, and β -catenin (Efstathiou et al., 1999). And in TFF3-transfected cells the amount of E-cadherin is reduced, accompanied by the reduction of α - and β -catenin levels followed by a reduction of the E-cadherin half-life in the TFF3-transfected cells (Meyer zum et al., 2004). Thus, we hypothesize that TFF1 might have an effect to mediate the expression of E-cadherin and β -catenin *in vitro* and *in vivo*.

1. 6. Objectives

Although the transcriptional regulation of TFF1 by E_2 has been well documented by a series of studies *in vitro*, its transcriptional regulation by E_2 is rarely verified *in vivo* and further rarely investigated using animal model. Therefore, the first objective of the project is to establish an *hTFF1-luc* transgenic rat model to investigate the hTFF1 promoter's regulation in the female reproductive organs.

Secondly, to date, most research on TFF1 has concentrated on its role in gastrointestinal wound healing and the promotion and migration of gastrointestinal carcinomas. TFF1 is originally identified as an estrogen-responsive gene in the MCF-7 human breast cancer cell line (Jakowlew et al., 1984), and is demonstrated to be expressed in the human and mouse uterus and vagina as well (Wiede et al., 2001; Masui et al., 2006; Lefebvre et al.,

1993; Rye et al., 1993). Therefore, we hypothesized that TFF1 might play an important role in uterine and vaginal epithelial cells through alteration of the expression of E-cadherin and β -catenin *in vivo*. For this purpose, we applied the TFF1 knock out mice model to investigate the impact of loss of TFF1 on the uterine and vaginal morphology, and its impact on the expression of E-cadherin and β -catenin.

CHAPTER 2: MATERIALS AND METHODS

2.1. Materials

2. 1. 1. Bacteria and plasmid

DH5 α	Invitrogen Life Technologies, Karlsruhe, Germany
E-cadherin promoter construct	Kindly provided by Dr. De Herreros
pGL3 vector	Invitrogen Life Technologies, Karlsruhe, Germany
β -galactosidase plasmid	Invitrogen Life Technologies, Karlsruhe, Germany

2. 1. 2. Antibodies

Mouse-anti-TFF1 (monoclonal)	Kindly provided by Dr. MC Rio
Rabbit -anti-ER α (MC-20, polyclonal)	Santa Cruz Biotechnology, Santa Cruz, USA
Mouse-anti-E-cadherin (monoclonal)	Transduction Laboratories, USA
Mouse-anti-E-cadherin (monoclonal)	BD Transduction Laboratories TM , USA
Goat-anti-luciferase (polyclonal)	Promega, USA
Mouse-anti-luciferase (monoclonal)	Upstate, USA
Mouse-anti- β -actin (monoclonal)	Sigma, Steinheim, Germany
Mouse-anti- β -catenin (monoclonal)	Santa Cruz Biotechnology, Santa Cruz, USA
Goat-anti-mouse Ig FITC (polyclonal)	Dakocytomation Denmark
Goat-anti-rabbit Ig G-FITC	Santa Cruz Biotechnology, Santa Cruz, USA
Donkey anti-goat Ig G-TR	Santa Cruz Biotechnology, Santa Cruz, USA
Goat anti-rabbit Ig G-TR	Santa Cruz Biotechnology, Santa Cruz, USA
Goat anti-rabbit Ig G-POD	BioGenes GmbH, Germany
Goat anti-mouse Ig G-POD	BioGenes GmbH, Germany
Donkey anti-rabbit IgG-HRP	Santa Cruz Biotechnology, Santa Cruz, USA
Anti-biotin antibody IgG-HRP	Cell Signaling, USA

2. 1. 3. Chemicals

X-gal	Carl Roth Karlsruhe, Germany
Dimethylformamide	Ferak, Berlin, Germany
Paraformaldehyde	Sigma, Steinheim, Germany
Ethanol	J.T. Baker, Netherland
17 β -estradiol	Sigma, Steinheim, Germany
ICI 182 780	Sigma, Steinheim, Germany
Tamoxifen	Sigma, Steinheim, Germany
Chloroforme	Sigma, Steinheim, Germany
Isopropanol	Sigma, Steinheim, Germany
DEPC	Sigma, Steinheim, Germany
Ponceau S	Sigma diagnostics, Steinheim, Germany
Triton X-100	Carl Roth, Karlsruhe, Germany

2. 1. 4. Reagents

DMEM medium	Invitrogen Life Technologies, Karlsruhe, Germany
Penicillin/streptomycin	Invitrogen Life Technologies, Karlsruhe, Germany
Fetal calf serum	Biochrom AG, Berlin, Germany
TRIZOL-Reagent	Gibco BRL, Karlsruhe, Germany
DNAase I	Invitrogen Life Technologies, Karlsruhe, Germany
Proteinase K	Macherey-nagel, Duren, Germany
Agarose	Gibco BRL, Life Technologies, Karlsruhe, Germany
QIA quick PCR purification kit	QIAGEN, Hilden, Germany
Mini-prep kit	QIAGEN, Hilden, Germany
Maxi-prep kit	QIAGEN, Hilden, Germany
Agarose gel DNA extraction kit	Roche, Mannheim, Germany
cDNA synthesis kit	Invitrogen Life Technologies, Karlsruhe, Germany
Radioimmuno assay kit	Diagnostic Products Corporation, Los Angeles, USA
BCA protein assay kit	Pierce, Bonn, Germany

GeneRuler™ 100bp DNA ladder	Fermentas
Nitrocellulose transfer membrane	Whatman GmbH, Germany
Phenol-Chloroform-Isoamylalcohol	Sigma, Steinheim, Germany
Tween-20	Carl Roth, Karlsruhe, Germany
Fugene 6 transfection reagent	Roche, Indianapolis, USA
Biotinylated protein ladder	Cell signaling, USA
Mouse serum	Dakocytomation Denmark
Albumin fraktion V	Carl Roth, Karlsruhe, Germany
BioTherm DNA polymerase	Rapidozym, Germany
Non-fat dry milk (blotting grade)	Bio-Rad, USA
pGEM T easy vector	Promega, USA
Complete Mini (CMR)	Sigma, Steinheim, Germany
Free fetal calf serum	Biochrom AG, Berlin, Germany
Chemiluminescence substrate	Pierce, Bonn, Germany
Oligotex TM mRNA Kit	QIAGEN GmbH, Germany
Epon resin	Plano, Marburg, Germany

2. 1. 5. Taqman Probes

Taqman Name /SYBR green	Sequence of Probe
Human β -actin	CACCCTTTCTTGACAAAACCTAACTTGCGC
Rat β -actin	CGATATCGCTGCGCTCGTCGTCG

2. 1. 6. Oligonucleotides

Primer Name	Genebank	
	Accession No	Sequences 5' - 3'
Mouse & rat β actin	NM_007393	GCCACCAGTTCGCCATGG GTCGTCCCAGTTGGTAACAATGC
Mouse E-cadherin	NM_009864	TGGACCGAGAGAGTTACCCTACATA ATTGCTGCTTGGCCTCAA
Human β -actin	X00351	ATCGTCCACCGCAAATGC TT CAACCGACTGCTGTCACCTTCA
Luciferase	pGL-3	TCATCGTTGACCGCCTGAAG AACTCCTCCGCGCAACTTTT
Human TFF1	NM_003225	TGGCCACCATGGAGAACAAG CACTGGGAGGGCGTGACA
Mouse & rat TFF1	D83231	CTGCCATGGAGCACAAGGT GGACACTGTCATCAAACAGCAA
Mouse TFF1	NM_009362	CCCCCGGGAGAGGATAAAT GGAGGGTGCCAAGTCTTGATG

2. 1. 7. Machines and Instruments

Spectrophotometer	UV-1202, SHIMADZU
Master Cycler Gradient	Eppendorf, Germany
ABI Prism 7700 SDS	Applied Biosystems, USA
Luminometer	Lumat LB 9507, Germany
Cooled IVIS® 100 Imaging system	Xenogen Corporation-Caliper, Alameda, CA; USA
Microplate reader	Bio-Rad, model 3550, Muench, Germany
Light microscopy	Axiopot, Zeiss, Göttingen, Germany
Transmission electron microscope	Zeiss EM10, Göttingen, Germany
Refrigerated Superspeed Centrifuge	Heraeus Kendro, USA
Immunofluorescence microscopy	Axiopot, Zeiss, Göttingen, Germany
Confocal microscope	Zeiss LSM 510, Göttingen, Germany

2. 2. METHODS

Human breast cancer cell line, MCF-7 cells (ER positive), was maintained in Dulbecco's MEM medium supplemented with 10% fetal calf serum, 1% glutamine, 100 U/ml penicillin, and 100 µg/ml streptomycin at 37°C and 5% CO₂.

2. 2. 1. Isolation of total RNA from cells and tissues

To study the transcriptional regulation of TFF1 by estrogen in vitro, Human breast cancer cell line, MCF-7 cells (ER positive), was cultured in phenol red-free Dulbecco's MEM medium supplemented with 5% charcoal-stripped fetal calf serum, 1% glutamine, 100U/ml penicillin, and 100µg/ml streptomycin at 37°C and 5% CO₂. After 3 days of culture, cells were treated with E2, ICI 182 780, tamoxifen, and combinations of these substances as indicated in table 4.

After treating the cells for 24 h, the total RNA was isolated from the cells using TRIZOL reagent. Specifically, MCF-7 cells were lysed directly in triplicate wells of 12-well plates by addition of 1 ml of TRIZOL reagent per well, and the cell lysate was passed several times through a pipette.

Afterwards, the cell lysate was transferred into 1.5 ml eppendorf tubes and incubated for 5 min at 15 to 30°C, and mixed with 0.2 ml of chloroform. The tubes were vigorously shaken by hand for 15 sec, incubated at 15°C to 30°C for 2-3 min, and centrifuged at no more than 12,000 g for 15 min at 2°C to 8°C. The aqueous phase was then transferred to a fresh tube and the RNA was precipitated from the aqueous phase by addition of 0.5 ml isopropanol. The RNA was incubated at 15°C to 30°C for 10 min and centrifuged at no more than 12,000 g for 10 min at 2°C to 8°C. The supernatant was removed, and the RNA pellet was washed once with 1 ml 75% ethanol. The RNA pellet was mixed by vortexing and centrifuged at no more than 7,500 g for 5 min at 2°C to 8°C. Finally, the RNA pellet was dried and dissolved in 20-50 µl 0.1% DEPC water.

To isolate the RNA from tissues, first the porcelain mortar and pestle were chilled using liquid nitrogen. 50-100 mg of the tissue was individually pulverized into a fine powder by hand grinding with the chilled porcelain mortar and pestle. Afterwards, the tissue powder was homogenized by addition of 1 ml of TRIZOL reagent. The remainder of the protocol was the same as described in the paragraph above.

RNA quality was determined by analyzing samples on 2% agarose gel, and the total RNA concentration and purity were determined by optical density measurements at 260 nm and 280 nm with a UV-1202 spectrophotometer.

2. 2. 2. Reverse transcription and polymerase chain reaction (RT-PCR)

Before a reverse transcription was performed, RNA samples were digested by DNAase I to remove DNA contamination by addition of 1 μ l DNAase I, 1 μ l 10 \times DNase I reaction buffer, 1 μ g RNA, and DEPC H₂O up to a total volume of 10 μ l. After incubating the samples for 15 min at room temperature, 1 μ l EDTA (25mM) was added and incubated for 10 min at 65°C to stop the digestion reaction. Afterwards, the 10 μ l RNA sample was added to the 10 μ l RT reaction solution prepared according to table 2. For each RNA sample, a negative control was prepared by omission of the Mu-LV-RT.

The single stranded cDNA (sscDNA) was synthesized by a random hexamer using a preamplification system as described in table 3 according to the following program: 21°C for 10 min followed by 37°C for 60 min, and 95°C for 10 min at the end of program in Master Cycler Gradient.

To perform the PCR reaction, 1 μ l of each sscDNA was used as a template to generate the PCR products with the primers according to the PCR reaction components shown in table 3.

The primer sequences of various genes were given in 2. 1. 5 Oligonucleotides. The PCR reactions were performed in the Master Cycler Gradient with the program of 95°C for 3 min followed by 24 cycles of 95°C for 30 sec, 60°C for 1 min and 72°C for 30 sec. At the

end of the PCR program, the reaction was extended for 6 min at 72°C. Aliquots of PCR products were analysed by electrophoresis in 2% agarose.

Table 2. Reverse transcription reactions

RT positive	Volume	RT negative	Volume
5×buffer	: 4 µl	5×buffer	: 4 µl
DTT (100µM)	: 0.5µl	DTT (100µM)	: 0.5µl
Random Hexamer	: 1µl	Random Hexamer	: 1µl
Mu-LV-RT (200 U/µl)	: 1µl	Mu-LV-RT (200 U/µl)	: —
RNAsin (40 U/µl)	: 0.5µl	RNAsin (40 U/µl)	: 0.5µl
dNTPs(10 mM each)	: 1µl	dNTPs(10 mM each)	: 1µl
RNA solution	: 10 µl	RNA solution	: 10 µl
DEPC H ₂ O	: up to 20µl	DEPC H ₂ O	: up to 20µl
Total volume	: 20 µl	Total volume	: 20 µl

Table 3. PCR reaction components

PCR reagents	Volume
10× Buffer	: 2.5 µl
MgCl ₂	: 1.0 µl
Sense primer (50 µM)	: 0.25 µl
Anti-sense primer (50 µM)	: 0.25 µl
Taq polymerase	: 0.25 µl
dNTP(10 mM)	: 0.25 µl
cDNA	: 0.50µl
dd H ₂ O	: 20 µl
Total volume	: 25 µl

2. 2. 3. Quantitative real-time PCR analysis

The absolute RNA amount was quantified by real-time PCR using the standard curve method. The plasmid DNA, which contained the target gene, was used to serve as the standard DNA concentration in the real-time PCR reaction to generate the standard curve.

2. 2. 3 .1 Construction of the target DNA plasmids

To obtain the plasmid DNA which contained the target gene, RT-PCR was performed as described in section 2.2.2 to obtain the target cDNA fragment. After the target cDNA fragment was generated and purified by a QIAGEN quick PCR purification kit on silica columns, the target cDNA fragment was cloned into pGEM-T easy plasmid vector according to the following ligation reaction: 5 µl 2×ligation buffer, 3 µl PCR fragment solution, 1 µl pGEM-T easy plasmid and 1 µl T4 ligation enzyme, followed by incubation at 4°C over night.

2. 2. 3. 2. Transformation of DNA plasmid into DH5α competent cells

To obtain a large amount of the plasmid DNA, the plasmid was transformed into DH5α competent cells.

DH5α was cultured on LB-agar and LB liquid medium supplemented with antibiotics (ampicillin: 50 µg/ml medium).

LB liquid medium: 10 g NaCl, 5 g yeast extraction, 10 g peptone in 1 liter deionized H₂O.

LB medium for agar plate: 15 g agar in 1 liter LB liquid medium supplemented with 50 µg/ml ampicillin.

10 µl solution of DNA fragment ligated with pGEM-T plasmid from section 2. 2. 3 .1 was added to 100 µl of DH5α competent cells and mixed gently with a pipette. After incubating on ice for 10 min, the mixture of DH5α and fragment DNA-ligated pGEM plasmid was

subjected to incubation at 42°C for 45 sec followed by incubation on ice again for 2 min. Afterwards, 900 µl LB liquid medium (without antibiotic) was added to the DH5α mixture and incubated at 37°C for 1 h at a shaking speed of 2, 200 rpm. At the same time, 40 µl X-gal (400mg X-gal diluted in 10ml dimethylformamide) was added to an LB-agar plate (containing 50 µg/ml ampicillin) and the LB-agar plate was dried at 37°C. After culturing of the DH5α mixture at 37°C for 1 h, 100µl of the DH5α mixture was added and spread evenly on each of the X-gal-covered LB-agar plates. Afterwards, the LB-agar plate, which contained the transformed DH5α, was incubated at 37°C over night. The next day, the transformed positive bacteria clones (white clone) were selected from the negative clones (blue clones) and cultured in 5 ml LB medium (contained 50 µg/ml ampicillin) for 24 h at a shaking speed of 2200 rpm. After 24h, 1 ml of DH5α cells was used for a mini-preparation of pGEM plasmid DNA using the mini prep kit according to the manufacturer's instructions. After confirming the presence of the target gene in the pGEM plasmid by PCR, the DH5α cells were abundantly cultured again in 300-400 ml ampicillin-positive LB medium to obtain a large amount of plasmid DNA containing the target gene by maxi-preparation.

2. 2. 3. 3. Maxi preparation of DNA plasmid

After the DH5α cells multiplied in the LB medium, the plasmid DNA was prepared by a Maxi-Prep kit. Specifically, 300-400 ml bacterial culture medium was centrifuged for 15 min at 6,000 rpm at 4°C. The supernatant was discarded, and the bacteria pellet was carefully resuspended in 20 ml P1 buffer. Afterwards, the bacteria contained in P1 buffer was transferred quickly to the 50 ml conical tubes (10 ml P1-bacteria-suspension/tube) followed by the addition of 20 ml P2 buffer (10 ml/tube), mixed and incubated at room temperature for 5 min. 20 ml of the prechilled P3 buffer (10ml/tube) was then added to the mixed buffer, mixed and incubated for 20 min on ice, and centrifuged for 30 min at 13,000 rpm.

At the same time, the column (provided by the company) was equilibrated by applying 10 ml QBT. After centrifugation, the supernatant was transferred to the column until it flowed up through the column completely. Afterwards, 30 ml of buffer QC was applied to the

column to rinse the plasmid DNA. The DNA plasmid was eluted by addition of 15 ml QF to the column. After the plasmid DNA was collected in buffer QF, 10.5 ml of isopropanol was added to buffer QF followed by centrifugation for 60 min at 4,000 rpm at 4°C to generate the plasmid DNA pellet. After the supernatant was discarded, the plasmid DNA pellet was washed with 1 ml 75% ethanol and centrifuged at 12,000g for 10 min at 4°C to remove the supernatant. After the pellet was air-dried at room temperature, the plasmid DNA was resuspended in 200-350 µl H₂O. The plasmid DNA concentration was measured by optical density spectrophotometry. Afterwards, the plasmid DNA was verified by PCR to confirm the presence of the target PCR product.

2. 2. 3. 4. Quantitative real-time PCR analysis

Real-time PCR amplifications were always performed by using a ABI Prism 7700 SDS (Applied Biosystems) in triplicate. PCR amplifications were performed in a total volume of 25 µl, which contained 0.5-1.0 µl cDNA sample, 1000 µM dNTPs, 3-9 mM MgCl₂, 100-900 nM of each primer, 100 nM taqman probe or 1 × SYBR green, and 1.25 U taqpolymerase with the following conditions: 3 min at 94°C, followed by a total of 39 cycles of 1 min at 60°C, 30 sec at 72°C and 30 sec at 94°C. The variables most likely to affect PCR efficiency are concentrations of MgCl₂, primer, and taqman probe. Therefore, it was necessary to optimize the real-time PCR reactions with different concentrations of the taqman probe or SYBR green, primer and MgCl₂ concentration.

After optimizing the real-time PCR conditions, DNA plasmid, which contained the target PCR product, was diluted into a ten-fold serial dilution (from 10 ng/µl to 10⁻⁴ ng/µl) to serve as the standard plasmid DNA concentration to generate a standard curve in each real-time PCR reaction for the calculation of PCR efficiency and quantification. The standard curve was constructed for each amplicon by plotting the cycle number (Ct) at which the amount of target DNA in standard dilution reaches a fixed threshold against the log of the amount of starting target cDNA. Absolute quantification of target amplicons in the samples was performed by interpolation of the threshold cycle number (Ct) against the corresponding standard curve. The resulting threshold cycle (Ct) values in the

standard curve for each input amount of template were plotted as a function of the \log_{10} concentration of input amounts and a linear trend-line was fitted to the data. The resulting slope of the line fitted to the data was used to determine the PCR efficiency as shown in the following equation. An ideal slope should be -3.32 for 100% PCR efficiency (100% meaning that the amount of template was doubled after each cycle). Deviations from 100% efficiency can be calculated by putting the value for the slope (S) into the following equation: PCR efficiency= $(10^{(1/-S)})-1$. Optimal standard curves were based on PCR amplification efficiency from 90 to 100% as demonstrated by the slope of the standard curve equation. Linear regression analysis of all standard curves showed a high correlation (R^2 coefficient ≥ 0.98) to be considered suitable for quantitative analysis of gene levels.

To minimize interassay variability, the same serial dilution of a standard plasmid DNA was used for all samples analyzed from a single experiment. Correction for inefficiencies in RNA input or reverse transcriptase was performed by normalization to the housekeeping gene β -actin.

2. 2. 4. Western blot

2. 2. 4. 1. Total protein preparation from cells and tissues

After washing with PBS, the cells were collected by centrifugation and resuspended in 150 μ l of CMR buffer. To prepare the protein solution from tissues, first the porcelain mortar and pestle were chilled using liquid nitrogen. Frozen tissues were individually pulverized into a fine powder by hand grinding with the chilled porcelain mortar and pestle. The powder was homogenized in 150-500 μ l of CMR buffer.

Subsequently, the samples were subjected to ultrasound in an ice water bath for 20 min, and centrifuged for 30 min at 4°C at 20,800 g. The supernatant (protein phase) was carefully transferred to chilled tubes with holes in the lids. After the protein content was measured using the BCA protein assay kit, all protein samples were frozen at -80°C for further experiments.

2. 2. 4. 2. Quantitative analysis of protein content

The total protein content was measured using the BCA protein assay kit according to the following protocol: 4 µl of protein solution was diluted in 36 µl CMR buffer, and serial dilutions of BSA standard and CMR buffer (served as blank) were added into the 96-well microplate with 10 µl per well in triplicate, respectively. Next, 200 µl of BCA working reagent (Regent A: B=50: 1) was added to each well. After the plate was incubated at 37°C for 30 min, the 96-well microplate was read at 540 nm by the microplate reader. The total protein concentration was calculated automatically by the computer based on the standard curve.

CMR buffer preparation: one tablet of CMR was dissolved in 10 ml of 50 mM Tris HCl-buffer, pH 7,4 with 200 µl 10 mM sodium orthovanadate.

2. 2. 4. 3. Western blot analysis

80 µg of protein per lane was separated by 10% SDS-PAGE (for TFF1, 12% SDS-PAGE gel was used) in running buffer and then electrotransferred onto nitrocellulose membranes using semi-dry buffer. The quality of protein blots was determined by Ponceau S staining of the nitrocellulose membranes. Afterwards, the nitrocellulose membranes were blocked for 1 h with non-fat dried milk. Membranes were washed in 0.1% Tween-20 Tris-buffered saline (TTBS; pH 7.5) twice, for 10 min each time, and rinsed in Tris-buffered saline (TBS; pH 7.5) twice, for 10 min each time. Subsequently, the membranes were incubated overnight with one of the following first antibodies: anti-Luciferase at 1:1000 dilution, anti-ER α at 1:200 dilution, anti-hTFF1 at 1:100 dilution, anti-E-cadherin at 1:1000 dilution, anti- β -catenin at 1:200 dilution, and anti- β -actin at 1:10,000 dilution, respectively, in TBS containing 0.5% NFDM. After being washed in 0.1% TTBS and TBS, blots were incubated with goat anti-mouse peroxidase-conjugated antibody at 1:1000 dilution or goat anti-rabbit peroxidase-conjugated antibody at 1:1000 dilution in TBS containing 0.5% NFDM. Blots were rinsed a final time, and the immune complexes were visualized with the chemiluminescence, SuperSignal® West Pico

chemiluminescent substrate.

10 fold running buffer (pH 8.3) : 30 g Tris base (MW 121.14), 144 g Glycine, 10 g SDS,
adjust the pH and add distilled water up to 1000 ml

1 fold semi-dry buffer: 5.8 g Tris base, 2.9 g Glycine, 0.37g SDS, 200ml
Methanol, add distilled water up to 1000 ml

10 fold TBS: 80 g NaCl, 2.0 g KCl, 30.0 g Trisbase, and adjust the
pH to 8.0 with 1 – 4 N HCl, Fill up to 1000 ml with
distilled water.

1X TBS 0.1%Tween Add 0.5 ml of Tween to 500 ml 1xTBS

2. 2. 5. Laser scan confocal microscopy and immunofluorescence analysis

MCF-7 cells were maintained in phenol red-free Dulbecco's MEM medium with 5% charcoal-stripped fetal calf serum for three days until the cells were grown to confluence. 19.5×10^5 cells were then seeded in a 12-cm diameter dish, which contained coverslips to allow the cells to grow on. After treatment, the cells were washed with PBS, fixed with pH 7.4 paraformaldehyde followed by incubation with 0.1% Triton X-100 for 5 min and 8% bovine serum albumin for 30 min.

The cells were then incubated with 2.5% mouse serum for 20 min followed by incubation of the primary antibody raised against TFF1 with a dilution of 1: 50, ER α with a dilution of 1: 100 (for confocal microscopy, anti-hTFF1 and anti-ER antibodies were added simultaneously), E-cadherin, β -catenin and luciferase with a dilution of 1: 100, respectively, and incubated at 4°C overnight. After washing with PBS, the binding of primary antibodies was detected with polyclonal goat anti-mouse Ig G-FITC or goat anti-rabbit IgG-TR diluted 1: 50 in PBS (for confocal microscopy, polyclonal goat anti-mouse IgG-FITC and goat anti-rabbit IgG-TR antibodies were added simultaneously at 1:50 dilution), and incubated for 60 min at room temperature.

Negative controls were performed by omission of the primary antibodies. Cells were washed and slides were mounted in vectashield and viewed through a laser scan confocal microscope.

To perform immunofluorescence in tissues, tissues were fixed in methacarn solution and embedded in paraffin after being harvested from the animals. The tissues were cut into 3 μm sections and mounted on superfrost glass slides for immunofluorescence staining. After the sections were deparaffinized in 100% xylol, 100% ethanol, 96% ethanol, 75% ethanol and PBS, respectively for 10 min, antigenic epitopes were demasked by boiling the sections in 10 mM citrate buffer (pH 6.0) for 20 min in a normal pressure cooker followed by the incubation of 0.1% Triton X-100 for 5 min and 8% bovine serum albumin for 30 min. Sections were reacted with the following specific primary polyclonal antibodies: mouse-anti-E-cadherin and mouse-anti- β -catenin, each at a 1:100 dilution overnight at 4°C. After washing with PBS, the binding of primary antibodies was detected with polyclonal goat anti-mouse Ig G-FITC diluted 1: 50 in PBS and incubated for 60 min at room temperature. Sections were washed and slides mounted in vectashield and viewed through an immunofluorescence microscopy.

Methacarn solution:

methanol: chloroform: acetic acid = 60%: 30%: 10%(v/v)

2. 2. 6. Transient transfection assays

A transient transfection assay was performed using Fugene 6 transfection reagent following the manufacturer's instructions. Briefly, cells were maintained in Dulbecco's MEM medium (phenol red-free) with 5% charcoal-stripped fetal calf serum, 100 U/ml penicillin, and 100 $\mu\text{g}/\text{ml}$ streptomycin at 37°C and 5% CO_2 for 3 days until the cells were grown to reach confluence. Afterwards the cells were seeded in 12 well plates ($2.5 \times 10^5/\text{well}/\text{ml}$ medium). After the cells grew to 50-80% confluence in 24 h, the medium was removed, and fresh medium was added after the cells were washed with PBS three

times. To transfect the cells, 100 μ l Optimen and 1.5 μ l Fugene 6 per well were mixed in a sterile tube and tapped gently to mix. The mixture was incubated at room temperature for 5 min. Afterwards, 0.5 μ g plasmid vector (hTFF1-pGL3 vector or E-cadherin promoter and ER α plasmid) and 0.5 μ g pSV β galactosidase (for standardizing the transfection efficiency) per well were added into the Optimen and Fugene 6 mixture, and mixed gently followed by incubation at room temperature for 15 min. 100 μ l mixed transfection solution per well was then added into the fresh medium in 12-well plate and the cells were incubated at 37 °C and 5% CO₂.

2. 2. 7. Luciferase and β galactosidase assay

Luciferase and β galactosidase activity were measured as described by Funke-Kaiser (Funke-Kaiser et al., 2003). Briefly, the medium was removed from the 12-well plate. After the cells were washed with PBS three times, the cells were dried at 37°C for 20 min, followed by the addition of 300 μ l lysis buffer per well and shaken for 20 min in a shaker. Afterwards, total cell lysates were generated by centrifugation at 14,000 rpm for 5 min. To measure the luciferase activity, 20 μ l of the cell lysates was used, and 100 μ l of luciferase substrate was added by the luminometer injection and the sample relative light units (RLU) were recorded for 20 sec using a luminometer. To measure the β -galactosidase, 50 μ l of the cell lysate was incubated at 48°C for 50 min. Subsequently, 70 μ l reaction buffer (diluted by Galacton Tropix and Galacto Reaction Buffer with a ration of 1:100) was added to 10 μ l of incubated cell lysate with an interval of 20 sec between samples. After incubating at room temperature for 30 min, the mixture solution was subjected to measurement of RLU. Luminescence was measured every 20 sec using a luminometer. The treated group cells were measured in triplicate. The luciferase RLU was normalized to that of β -galactosidase.

2. 2. 8. Establishment of the *hTFF1-luc* transgenic rat model

2. 2. 8. 1. Construction of the hTFF1 promoter-luciferase pGL3 vector

The plasmid hTFF1-pGL3 was constructed by PCR amplification of the 5'-flanking region

of the human TFF1 promoter. Following the amplification, the resulting 1000-bp PCR product was ligated into pGEM-T easy vector using the TA-cloning kit (see section of 2. 2. 3 .1). The 1000-bp PCR product was released from the pGEM-T easy vector by restriction enzymes and subcloned upstream of the cDNA encoding firefly luciferase in the pGL3-vector, because the pGL3-vector contains modified luciferase complementary DNA and simian virus 40 polyadenylation signal, which results in much higher luciferase expression. To further verify whether the hTFF1-pGL3 construct could be regulated by E₂, the functional response of the hTFF1-pGL3 construct to E₂ was examined by transient transfection of MCF-7 cells.

2. 2. 8. 2. Transient transfection assays

To verify whether or not the new hTFF1-pGL3 construct will be E₂-dependently regulated so that it can qualify to be used to generate a transgenic rat model, a transient transfection assay was performed as described in section 2.2. 6. After 24 h of the transfection, the MCF-7 cells were treated with a series of concentration of E₂ (10⁻¹², 10⁻¹¹, 10⁻¹⁰, 10⁻⁹, 10⁻⁸, 10⁻⁷ M). Each concentration was carried out in triplicate. The luciferase activity was measured as described in section 2.2.7.

2. 2. 8. 3. Generation of the *hTFF1-luc* transgenic rats

After examination of the functional response of the hTFF1-pGL3 construction to E₂, fusion genes consisting of portions of the hTFF1 promoter and a luciferase reporter gene (hTFF1-luciferase) were released from hTFF1-pGL3 by restriction enzymes. The linearized fragment (Fig. 6.) was separated by agarose gel electrophoresis, isolated with an agarose gel DNA extraction kit and further purified. To generate the *hTFF1-luc* transgenic rat model, the purified DNA fragment was microinjected into the pronucleus of fertilized Sprague-Dawley (SD) rat eggs and transplanted into the oviduct of pseudopregnant SD rats (which have been mated with a vasectomized male, the mating act can initiate a physiological change in the female which stimulated the development of the implanted embryos). The microinjected *hTFF1-luc* transgene randomly integrates into

the chromosomal DNA at nicks, usually at a single site. Genomic DNA was isolated from the tails of the offspring of the pseudopregnant SD rats for PCR analysis to detect the presence of the TFF1-luciferase transgene. Those TFF1-luciferase transgene positive rats confirmed by PCR were identified as transgenic founder rats.



FIG. 6. Schematic diagram of the human TFF1-luciferase fragment

2. 2. 8. 4. Identification of the founder generation

Genomic DNA was extracted from tailcuts from offsprings by the following protocol:

30 μ l of proteinase K and 600 μ l of tail buffer were added to the tailcut tissues followed by incubation at 55–56°C until the tail tissues were completely dissolved. Afterwards, 500 μ l phenol-chloroform-isoamylalcohol 25:24:1 was added to the tailcuts mixture solution, vortexed vigorously and incubated for 10 min on ice followed by centrifugation for 15 min at 20,800 g. The aqueous phase was transferred into a new eppendorf tube and 60 μ l of 3 M sodium-acetate plus 600 μ l ice cold (-20°C) isopropanol were added. The tubes were inverted gently several times followed by incubation at -20°C overnight. DNA pellets were generated by centrifugation for 10-15 min at 10,000–11,000 g, and then washed with 800–1000 μ l ice cold (-20°C) 80% ethanol. Subsequently, the DNA pellets were dried and diluted with 20-50 μ l H₂O and the DNA concentrations were measured by optical density measurements at 260 and 280 nm.

50 ng genomic DNA was applied as a template to identify the *hTFF1-luc* transgene in the transgenic founder rats and their offspring by PCR analysis using the luciferase-specific primers: 5'-TCATCGTTGACCGCCTGAAG-3' (forward primer) and 5'-AACTCCTCCGCGCAACTTTT-3' (reverse primer). The PCR program was 95°C for 3 min followed by 34 cycles of 95°C for 30 sec, 60°C for 1 min and 72°C for 30 sec. At the

end of the PCR program, the reaction extended for 6 min at 72°C. Aliquots of PCR products were analyzed by electrophoresis in 2% agarose.

2. 2. 8. 5. Generation of the *hTFF1-luc* heterozygous and homozygous transgenic rat lines

After the luciferase positive rats (transgenic rat founders) were identified, the female transgenic rat founders were bred with wild type SD rats to generate *hTFF1-luc*^{+/-} (heterozygous) transgenic rat lines. The *hTFF1-luc*^{+/-} rats were then inbred to produce the homozygous (*hTFF1-luc*^{+/+}) transgenic rats. We identified *hTFF1-luc*^{+/+} transgenic rats using the classic Mendel's Equal Segregation Law after backcrossing each of the *hTFF1-luc* transgenic rats onto nontransgenic background (SD) rats. If all the offspring were positively identified by PCR for the presence of *hTFF1-luc* transgene, the transgenic rat could be considered *hTFF1-luc*^{+/+} rat. All the transgenic rats were generated and maintained in accordance with the Guide for the Care and Use of Laboratory Animals from the physiological society of Germany and Landesamt for Gesundheit und Soziales Berlin (LAGeSo; Registration numbers: 0253/04 and 185/99).

2. 2. 9. Estrous cycle determination and sacrifice of the *hTFF1-luc* transgenic rats

To determine the estrous cycle phase, vaginal smears were taken from female *hTFF1-luc* transgenic rats. Thus, the animals were killed by decapitation at 09:00 AM. Blood and tissues were harvested from the transgenic rats for further experiments.

2. 2.10. *In vivo* bioluminescent imaging

To further confirm promoter activity *in vivo* and to characterize the approximate organ regeneration of the transgene, *in vivo* bioluminescent imaging was performed as previously described by Zhang (Zhang et al., 2004). Briefly, *in vivo* bioluminescent imaging was performed using the cooled IVIS® 100 Imaging system linked to a PC running Living Imaging (Xenogen Corporation-Caliper) and IGOR software (Wavemetrics, Seattle, WA, USA) under Windows XP (Fig.7). The IVIS system consists of a cooled CCD

camera mounted on a light-tight specimen chamber, a cryogenic refrigeration unit, a camera controller, and a computer system for data analysis. This system provides high signal-to-noise images of luciferase signals emitted from within living animals. The luciferase enzyme produces light in the presence of the substrate luciferin, oxygen and ATP. The light produced penetrates into mammalian tissues and can be externally detected and quantified using sensitive light-imaging systems. Luciferin, the substrate, was injected into the intraperitoneal cavity at a dose of 150 mg/kg body weight (30 mg/ml luciferin) 5 min prior to imaging. The female *hTFF1-luc* transgenic rats were anesthetized with isoflurane/oxygen and placed on the imaging stage. Imaging began 5 min after the administration of luciferin. Dorsal images were collected for one second using the IVIS Imaging System. The distance of the rat from the CCD camera was always the same. Photon flux data were normalized for differences in the image acquisition time. Signal intensity was quantified as the flux of all the detected photon emissions within the region of interest of the rat body using living Image software.



FIG. 7. Schematic picture of the IVIS 100 Imaging System

2. 2. 11. RT-PCR to identify the tissue-specific expression of the luciferase transgene in *hTFF1-luc* transgenic rats

After isolating the total RNA from tissues, the mRNA was isolated using the OligotexTM mRNA Kit according to the manufacturer's instructions. The mRNA concentration and purity were determined spectrally before reverse transcription (RT). RT reaction and PCR were performed as described in section of 2. 2. 2 in a thermal cycler PCR machine.

2. 2. 12. Luciferase enzyme activity assay in *hTFF1-luc* transgenic rats

Analysis of *in vitro* luciferase activity in different tissues is considered to be a good indicator of the integration of *hTFF1-luc* gene and of the actions of ligand toward activation of the hTFF1 promoter. To precisely determine the hTFF1 promoter regulation in tissues of the *hTFF1-luc* transgenic rats, luciferase activity assay *in vitro* was performed as described by Manthorpe (Manthorpe et al., 1993). Briefly, mortar and pestle were chilled in advance by liquid nitrogen. Frozen organs were individually pulverized into fine powder using the chilled mortar and pestle. Afterwards, 300 µl of "lysis buffer" was added to each powder sample. The samples were vortexed for 15 min (using a multitube platform and Genie mixes form Fisher) followed by freezing and thawing 3 times alternating between liquid nitrogen and 37°C water baths. The supernatant was generated by centrifugation at 10,000 g for 30 min and transferred into new 1.5 ml eppendorf tubes. The extraction process was repeated (without freeze-thawing) after adding another 300 µl of lysis buffer to each sample pellet. The samples were vortexed and centrifuged at 10,000 g for 30 min again. The second supernatant was combined with the first one to generate the whole supernatant. Afterwards, 20 µl of the extract supernatant for each sample was immediately assayed for luciferase activity by the addition of 100 µl luciferin substrate using the luciferase assay system. Luminescence was measured as relative light units (RLU) for 20 sec using a luminometer. The RLU were normalized to the protein content.

2. 2. 13. Hormonal analysis

Blood was collected from killed *hTFF1-luc* transgenic rats and allowed to clot in an ice bath (4°C) for 2 h. Serum was collected after centrifugation and stored at -20°C until analysis. Serum estradiol and progesterone concentrations were measured using a double-antibody radioimmunoassay kit according to the manufacturer's instructions. Samples and standards were analyzed in duplicate, and the intra- and inter-assay coefficients of variations were less than 12%.

2. 2. 14. Estrous cycle determination and sacrifice of the TFF1 knock out mice

TFF1 knock out mice were established by Olivier Lefebvre (Lefebvre et al., 1996), and together with wild type mice (129/Svj), which served as a control, were held in our animal facility to investigate the function of TFF1 within the female reproductive organs. The mice were exposed to constant light/dark periods of 12 hours each, at a temperature of 21±1°C and 50±5% relative humidity.

The estrous cycles of the female TFF1 knock out mice (TFF1^{-/-}) and wild type mice (SV 129J as control group) were examined by vaginal smear for 21 consecutive days. The mice were killed to collect the blood from the aorta. The blood was allowed to clot in an ice bath (4°C) for 2h. Serum was collected after centrifugation and stored at -20°C until later analysis.

The uterus, vagina and stomach (serve as a positive control for TFF1) were harvested from the TFF1 knock out mice. Each organ was cut into three parts, one of which was put into the liquid nitrogen immediately for RNA isolation and protein preparation for western blot analysis. Another part was kept in the methacan solution for immunohistochemistry or immunofluorescence analysis and the remaining part was kept in a Karnovsky solution for electron microscopy analysis.

Karnovsky solution (100 ml): 15 ml 25% Glutaraldehyde, 45 ml 0.2 M phosphate buffer, 40 ml 3% paraformaldehyde

2. 2. 15. Gross morphological and histological analysis of female reproductive organs in TFF1 knock out mice

After the organs were excised and fixed in methacarn solution, the tissues were embedded in paraffin and cut into 3 μm sections. Subsequently, the tissue sections were deparaffinized and rehydrated in distilled water. Afterwards, the dewaxed sections were stained with 1.0% wt/vol hematoxylin and 0.5% wt/vol eosin. The histopathological changes were examined using light microscopy.

2. 2. 16. Measurement of the thickness of epithelial layer

We hypothesized that TFF1 might play an important role in uterine and vaginal epithelial cells through alteration of the expression of E-cadherin and β -catenin in vivo, which play important roles in the epithelial cell-cell adhesion. Therefore, we deduced that loss of TFF1 might have an impact on the thickness of the epithelial layer. Thus, after staining the uterine and vaginal sections with hematoxylin and eosin, the histopathological changes were examined under light microscopy. The thickness of the total uterine and vaginal epithelial layers and uterine diameter were measured using the imaging set-up system and public domain Scion Image Analysis software (Scion image 1.62 c MacOs, Scion, Frederick, MD). Nine fields were randomly selected to analyze the thickness of uterine and vaginal epithelial layers from each section (three sections per animal, n= 4-6) in TFF1 knock out mice and wild type mice at estrous as well as diestrous phases.

2. 2. 17. Electron microscopy analysis

To further investigate the impact of the loss of TFF1 on the uterine and vaginal epithelial alterations in microstructure, electron microscopy analysis was employed. The uterus and vagina were kept in Karnovsky solution after being harvested from the TFF1 knock out mice. Tangential sections were made in the middle of the uterine and vaginal tissues using a razor blade. Subsequently, the tissues were cut crosswise for preparation of ultrathin sections. All samples were fixed in 1% glutaraldehyde plus 1% tannic acid in 0.1 M phosphate buffer (pH 7.4) and post-fixed in 1% OsO_4 in phosphate buffer. After rinsing

and dehydration in ethanol, the samples were embedded in Epon resin, cut with an Ultracut E and the sections were stained with 2% uranyl acetate/lead citrate. The specimens were examined under a transmission electron microscope.

2. 2. 18. Statistical analysis

Statistical analysis was performed with the Statistical Package for Social Sciences for Windows (SPSS; version 12.0) and Sigma Plot for Windows Version 9.0 (Systat Software GmbH) using the Mann-Whitney-U-test, and T-test. All data are expressed as mean \pm SD if not otherwise indicated and significance assigned at a value of $P < 0.05$.